Supporting Information

Experimental

Materials

PM6 was purchased from *Volt-Amp Optoelectronics Tech. Co., Ltd, Dongguan, China*. PNDIT-F3N were purchased from eFlexPV Limited. PEDOT:PSS (Clevios P VP 4083) was purchased from Heraeus Inc., Germany. All the other reagents and chemicals were purchased from Sigma Aldrich or Aladdin and used as received.

Experimental Equipment and Facilities

Device fabrication. Solar cells were fabricated in a conventional device configuration of ITO/PEDOT:PSS/active layer/PNDIT-F3N/Ag. The ITO substrates were cleaned by detergent and then sonicated with deionized water, acetone and isopropanol subsequently, and dried overnight in an oven. The glass substrates were treated with UV-Ozone for 30 min before PEDOT:PSS was spin-casted on top at 5,000 rpm for 30 s, and then annealed at 150 °C on a hotplate for 10 min in air.

(1) For the binary devices, namely, PM6:PY-V-*γ* and PM6:PYO-V, PM6 was dissolved in toluene (the concentration of donor was 8 mg mL^{-1}), PY-V-*γ* and PYO-V are also dissolved in toluene (the concentration of donor was 12 mg mL^{-1}) with 1-chloronaphthalene (2% vol) as an additive. Both solutions were stirred overnight in a nitrogen-filled glove box. The donor solution was spin-casted at 4000 rpm for 30 s onto the PEDOT:PSS films, then the acceptor solution was spin-casted at 4000 rpm for 30 s onto the donor films followed by a thermal annealing of 95°C for 5 min.

(2) For the ternary device, namely, PM6:PY-V-*γ*:PYO-V, PM6 was dissolved in toluene (the concentration of donor was 8 mg mL^{-1}), PY-V-*γ*:PYO-V=8:2 (wt%: wt%) was also dissolved in toluene (the concentration of donor was 12 mg mL^{-1}) but with 1-chloronaphthalene (2% vol) as an additive. Both solutions were stirred overnight in a nitrogen-filled glove box. The donor solution was spin-casted at 4000 rpm for 30 s onto the PEDOT:PSS films, then the acceptor solution was spin-casted at 4500 rpm for 30 s onto the donor films followed by a thermal annealing of 95°C for 5 min.

For all types of devices, a methanol with 0.5% vol acetic acid blend solution of PNDIT-F3N at a concentration of 0.5 mg mL^{-1} was spin-coated onto the active layer at 2000 rpm for 30s. Around 100 nm of Ag was evaporated under 4×10^{-4} Pa through a shadow mask. Then the encapsulation was carried out. The thickness of each layer in the device are measured as: PEDOT:PSS(30nm~50nm)/active layer(90nm~130nm)/PNDIT-F3N(~10nm)/Ag(100nm).

Device characterization. The current density-voltage (*J-V*) curves of all encapsulated devices were measured using a Keithley 2400 Source Meter under AM 1.5G (100 mW cm^{-2}) using an Enlitech solar simulator. The light intensity was calibrated using a standard Si diode with KG5 filter to bring spectral mismatch to unity. Optical microscope (Olympus BX51) was used to define the device area (7.2 mm^2), mask is 3.94 mm^2. EQEs were measured using an Enlitech QE-S EQE system equipped with a standard Si diode. Monochromatic light was generated from a Enlitech 300W lamp source.

Analysis and Characterisation

SCLC Measurements: The electron- and hole-mobilities were evaluated using the space-charge limited current (SCLC) method. The device architecture of the electron-only devices was ITO/ZnO/active layer/PNDIT-F3N/Ag and that of the hole-only devices was ITO/PEDOT:PSS/active layer/MoO_3/Ag. The charge carrier mobilities were determined by fitting the dark current into the model of a single carrier SCLC according to the equation: $J = 9\varepsilon_0\varepsilon_r\mu V^2/8d^3$, where J is the current density, d is the film thickness of the active layer, μ is the charge carrier mobility, ε_r is the relative dielectric constant of the transport medium, and ε_0 is the permittivity of free space. The V used in the equation is defined by: $V = V_{app} - V_{bi}$, where V_{app} is the applied voltage, V_{bi} is the built-in voltage. The carrier mobilities were calculated from the slope of the $J\sim V^2$ curves.

TR-PL characterizations: TR-PL measurements were carried out on encapsulated thin films. A 100 fs Ti:Sapphire oscillator (Coherent Mira 900) operating at 76 MHz repetition rate was tuned to 750 nm and focused to excite the sample. The PL was collected and guided into a spectrometer equipped with a silicon single-photon counter to carry out time-correlated single-photon counting (TCSPC), integrating the majority of the PL. Low-temperature measurements were carried out with the sample mounted

inside a helium flow cryostat with an active feedback temperature controller. The PL spectra were obtained using a Si photodiode array detector.

Film-depth-dependent light absorption spectroscopy (FLAS) and composition distribution: Film-depth-dependent light absorption spectra were acquired by an in-situ spectrometer (PU100, Shaanxi Puguang Weishi Co. Ltd.) (Shaanxi, China) equipped with a soft plasma-ion source. The power-supply for generating the soft ionic source was 100 W with an input oxygen pressure ~10 Pa. The film surface was incrementally etched by the soft ion source, without damage to the materials underneath the surface, which was in situ monitored by a spectrometer. From the evolution of the spectra and the Beer–Lambert's Law, film-depth-dependent absorption spectra were extracted.

The composition distribution along the film-depth direction was obtained from the film-depth-dependent spectra by fitting the sub-layer absorption using the absorption of the pure components. The exciton generation contour is numerically simulated upon inputting sub-layer absorption spectra into a modified optical transfer-matrix approach.

Transient photovoltage (TPV) and transient photocurrent (TPC) measurements: In TPV measurements, the devices were placed under background light bias enabled by a focused Quartz Tungsten-Halogen Lamp with an intensity of similar to working devices, *i.e.,* the device voltage matches the open-circuit voltage under solar illumination conditions. Photo-excitations were generated with an 8 ns pulses from a laser system (Oriental Spectra, NLD520). The wavelength for the excitation was tuned to 518 nm with a spectral width of 3 nm. A digital oscilloscope was used to acquire the TPV signal at the open-circuit condition. TPC signals were measured under short-circuit conditions under the same excitation wavelength without background light bias.

GIWAXS characterization: Grazing-incidence wide-angle X-ray scattering (GIWAXS) measurements were conducted at beamline BL16B1 at Shanghai Synchrotron Radiation Facility (SSRF). Data were acquired at the critical angle (0.13°)

of the film with a hard X-ray energy of 10 keV. X-ray irradiation time was 30 s, dependent on the saturation level of the detector. Samples were prepared on Si substrates using identical blend solutions as those used in devices. The coherence length was calculated using the Scherrer equation (7): CL = $2\pi K/\Delta q$, where Δq is the full-width at half-maximum of the peak and K is a shape factor (1 was used here).

R-SoXS Characterization: R-SoXS measurements were performed in transmission geometry with linearly polarized photons under high vacuum (1×10^{-7} Torr) at beamline 11.0.1.2 at the Advanced Light Source (ALS). The scattering 2D images were collected in a vacuum cooled 2D charge-coupled device (CCD) detector (Princeton Instruments, I-MTE, 2048×2048 pixels). The soft X-ray energies were tuned between 270 and 285 eV in the R-SoXS experiments. Using a custom Nika analysis package, 2D scattering patterns were reduced to 1D scattering profiles and normalized for the X-ray flux. Since distance travelled through the samples by the X-rays affects the scattering intensity, it was normalized for absorption and film thickness. Samples for R-SoXS measurements were first prepared on a polystyrene sulfonate (PSS) modified Si substrate and floating in water to a 1.5 × 1.5 mm, 100 nm thick Si3N4 membrane supported by a 5 × 5 mm, 200 um thick Si frame.

Stability test: The MPP tracking was measured using the solar cell stability test setup (MT-PV-16, Tianjin Meitong Corp., China) in an N_2 atmosphere, which was conducted under continuous 100 mW/cm^2 illumination provided by a white LED (MT-LED-80, Tianjin Meitong Corp., China), and the results were automatically recorded by the aging test software.

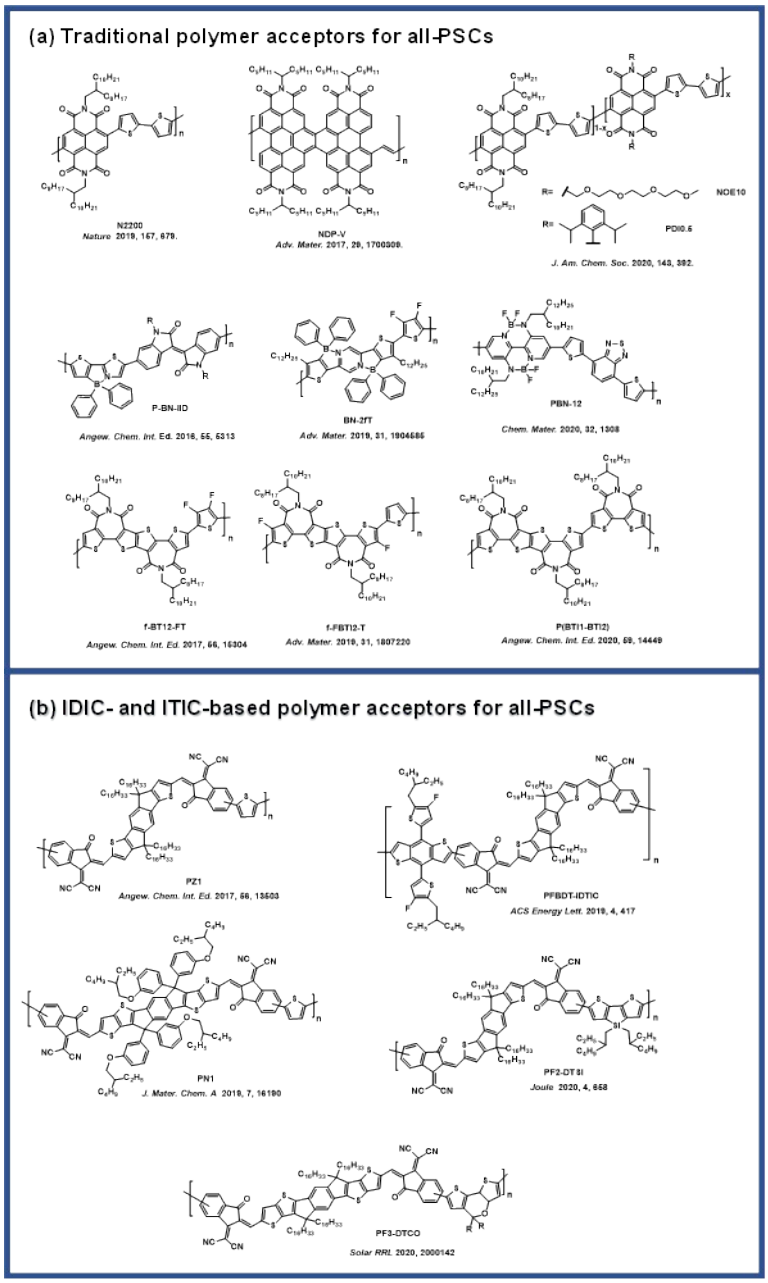

Figure S1. (a) Molecular structures of the traditional polymer acceptors in all-PSCs: naphthalene diimide, perylene diimide, B←N unit and bithiophene imide-based polymer acceptors. (b) Representative molecular structures of the IDIC- and ITIC-based polymer acceptors for all-PSCs.

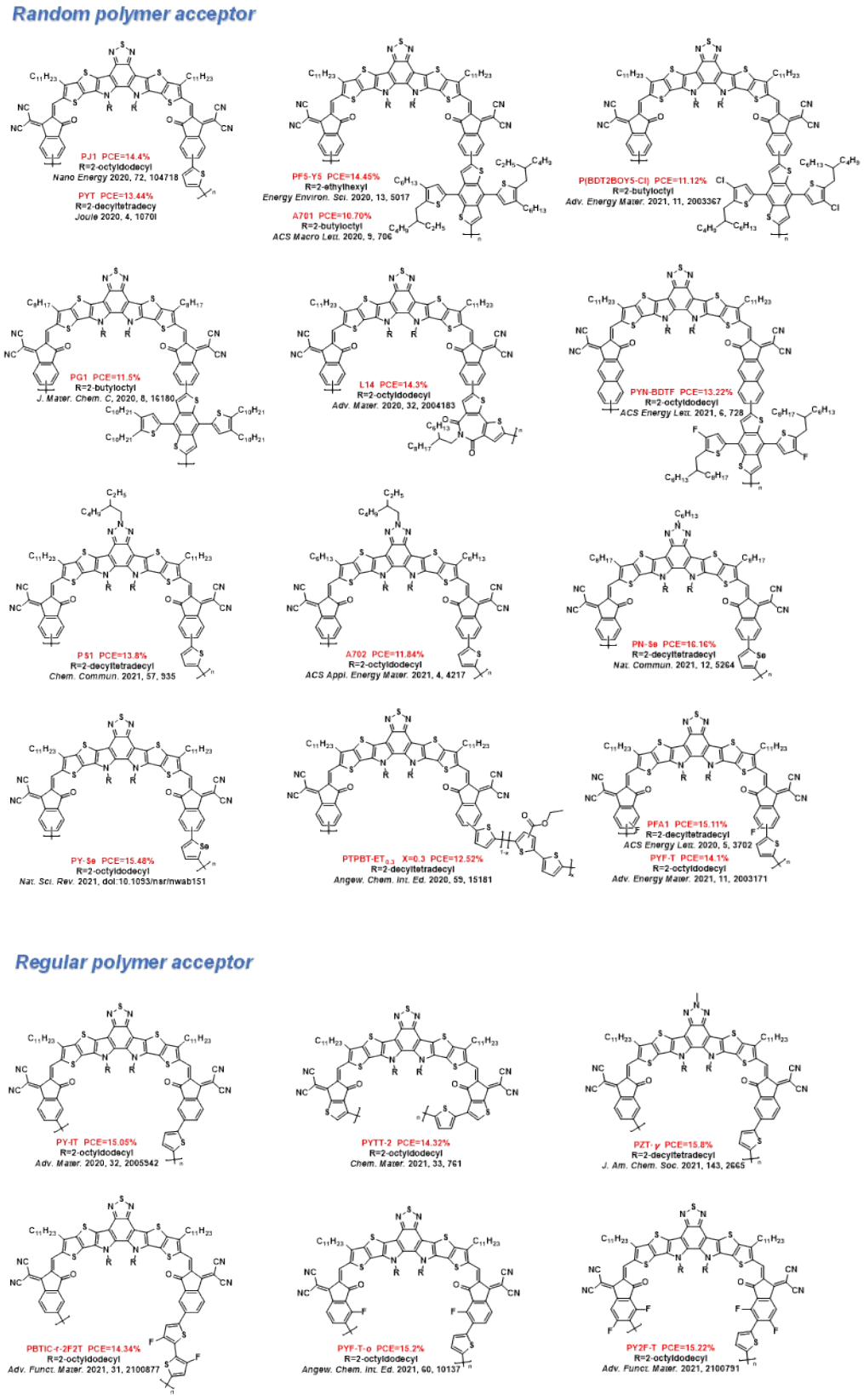

Figure S2. Molecular structures of Y-series polymer acceptors reported recently and the corresponding PCEs in the binary all-PSCs.

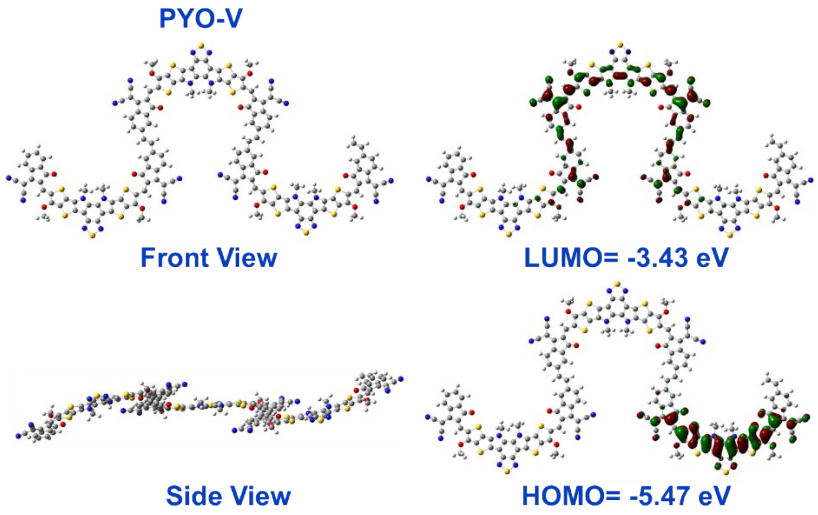

Figure S3. DFT calculation results of the PYO-V.

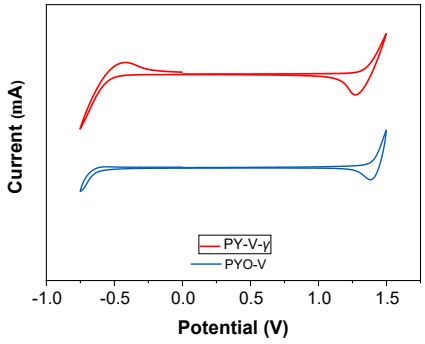

Figure S4. CV curves for PY-V-γ and PYO-V

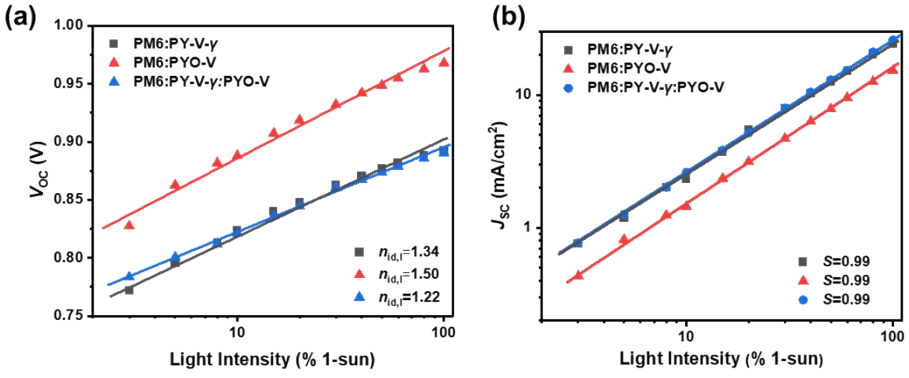

Figure S5. a) V_{OC} versus light intensity binary and ternary devices. b) J_{SC} versus light intensity of binary and ternary devices.

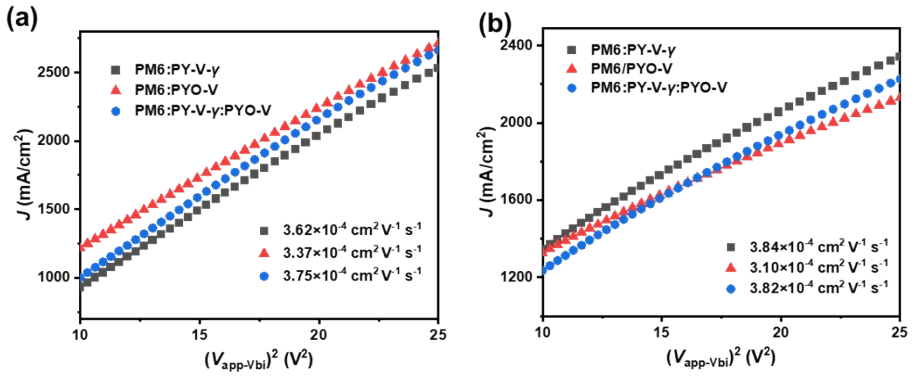

Figure S6. (a) Hole-only devices and (b) electronic-only devices of the three all-PSCs for mobility measurements.

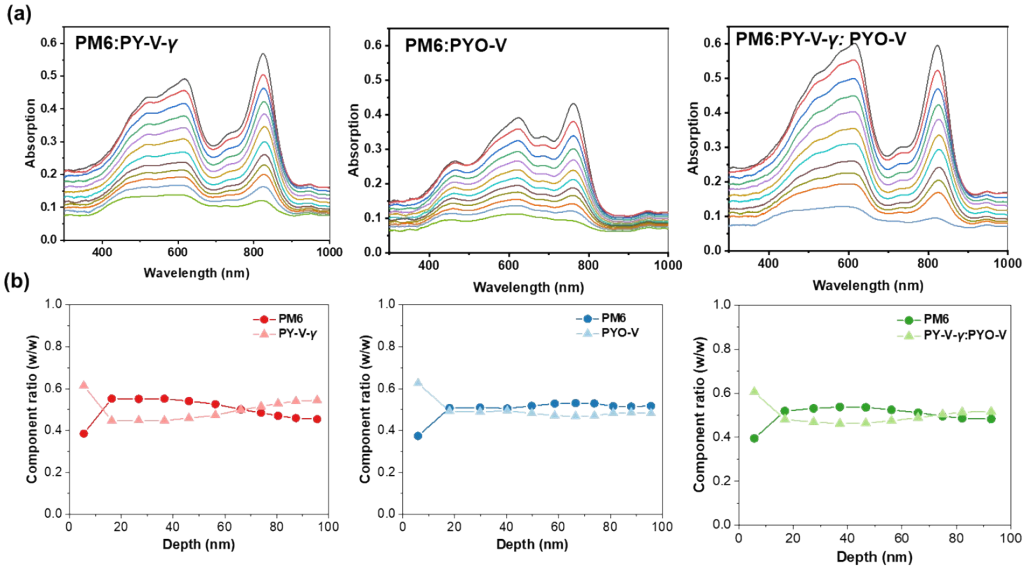

Figure S7. (a) Film-depth-dependent light absorption spectra. (b) The composition ratio across the vertical direction of the active layer.

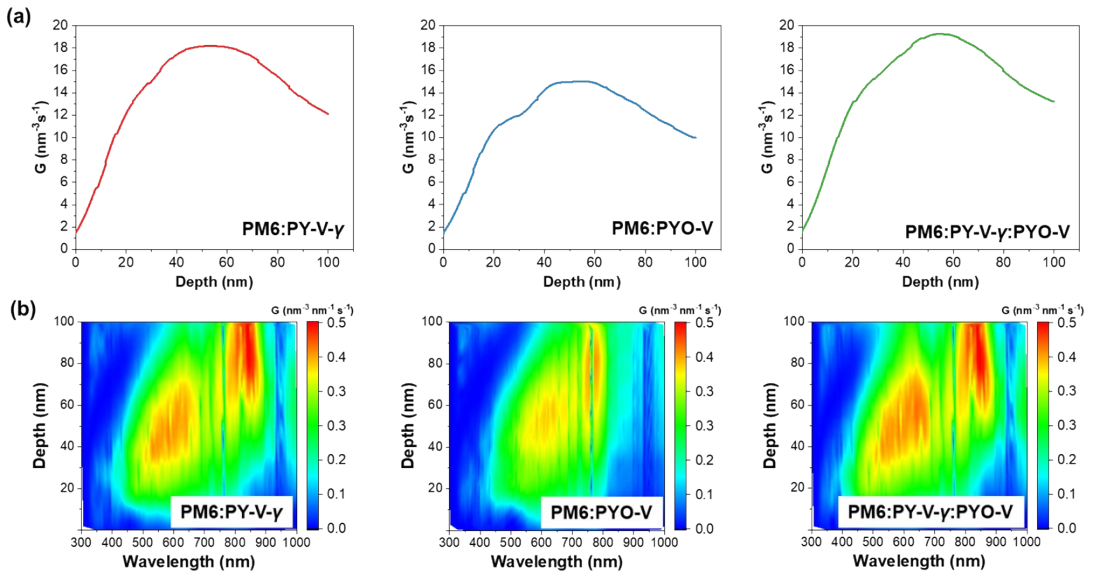

Figure S8. (a) Integrated generation rate in the vertical direction of the active layer. (b) Exciton generation map across the vertical direction of the active layer film as a function of wavelength.

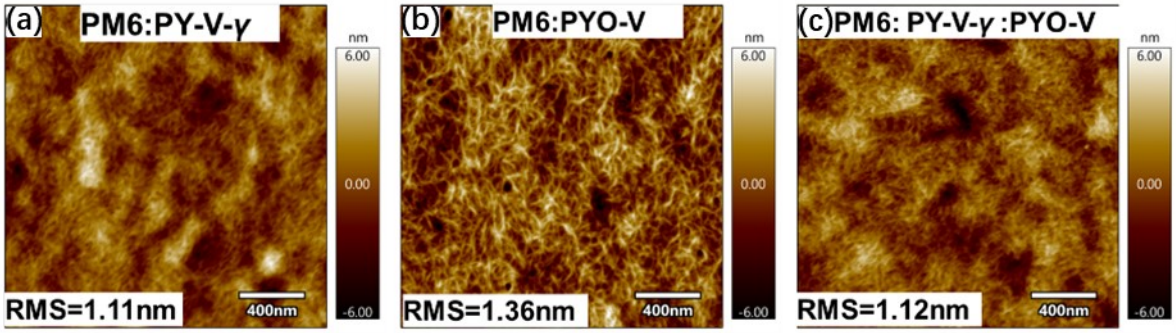

Figure S9. AFM images of of binary and ternary blend films.

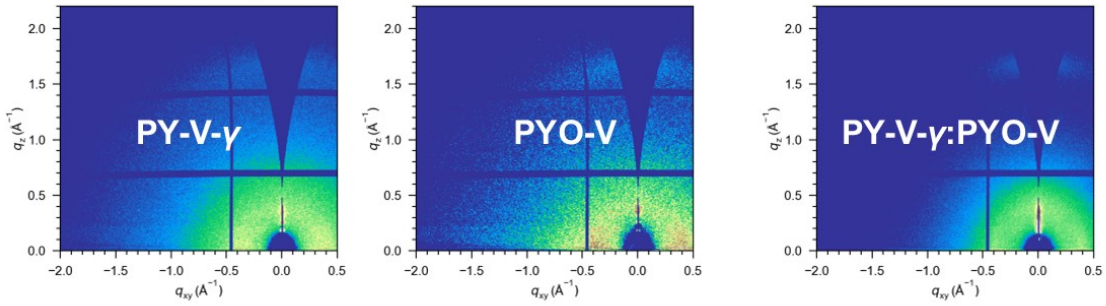

Figure S10. GIWAXS patterns of corresponding acceptor films.

Table S1. GIWAXS (100) and (010) peak parameters.

Active layer	100 distance [Å]	100 CL [Å]	010 distance[Å]	010 CL[Å]
PM6:PY-V-γ	18.7	54.3	3.62	23.6
PM6:PYO-V	19.2	56.0	3.63	23.1
PM6:PY-V-γ:PYO-V	18.8	62.1	3.62	25.1

Table S2. Morphology parameters extracted from the RSoXS measurements.

Sample	Peak#	q_{peak} (nm^{-1})	Long Period (nm)	ISI (a.u.)	FWHM (nm^{-1})
PM6:PY-V-γ	1	0.048	131	$3.55e^{-23}$	0.06
	2	0.195	32	$2.62e^{-22}$	0.29
PM6:PYO-V	1	0.076	83	$3.30e^{-22}$	0.19
PM6: PY-V-γ:PYO-V	1	0.049	128	$5.32e^{-23}$	0.06
	2	0.186	34	$2.57e^{-22}$	0.23

ISI – Integrated scattering intensity

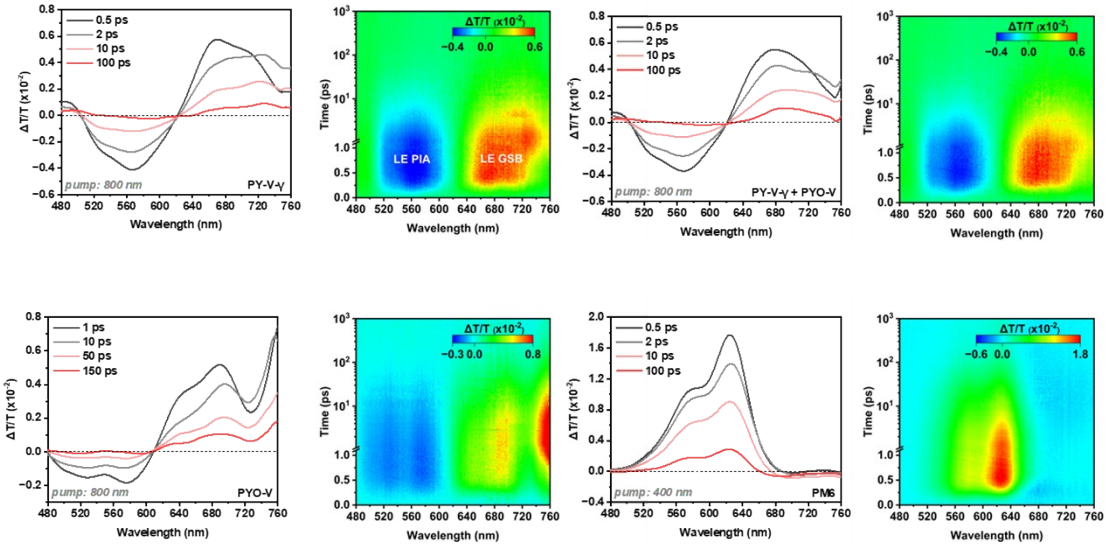

Figure S11. Spectral line cuts at specified pump-probe delay times and pseudo 2D maps of transient absorption for pure donor and pure acceptor thin films at a constant excitation fluence of 2 μJ/cm^2 with 800 nm pump wavelength. The local excitons (LE) photo-induced absorption (PIA) and ground state bleach (GSB) are also labelled.

Table S3. Detailed E_{loss} parameters of the OSCs based on the three all-PSCs.

active layer	E_g a) (eV)	V_{OC} SQb) (eV)	V_{OC} rad c) (eV)	V_{OC} (eV)	E_{loss} (eV)	ΔE_1 (eV)	ΔE_2 d) (eV)	ΔE_3 e) (eV)
PM6:PY-V-γ	1.422	1.160	1.111	0.909	0.514	0.262	0.050	0.202
PM6:PYO-V	1.542	1.271	1.188	0.968	0.574	0.271	0.083	0.220
Ternary	1.426	1.164	1.115	0.927	0.499	0.262	0.049	0.188

a) E_g: optical bandgaps, via the derivatives of the FTPS-EQE spectra (dEQE/dE)

b) Voc^{SQ}: Schokley-Queisser limit to V_{OC}.

c) Voc^{rad}: radiative limit to Voc, measured using EQE_{EL}

d) ΔE_2 (Voc^{SQ}-Voc^{rad}): voltage losses due to non-ideal absorption (it was calculated from EL and FTPS measurements).

e) ΔE_3 ($\Delta Voc^{non-rad}$): voltage losses due to non-radiative recombination only.

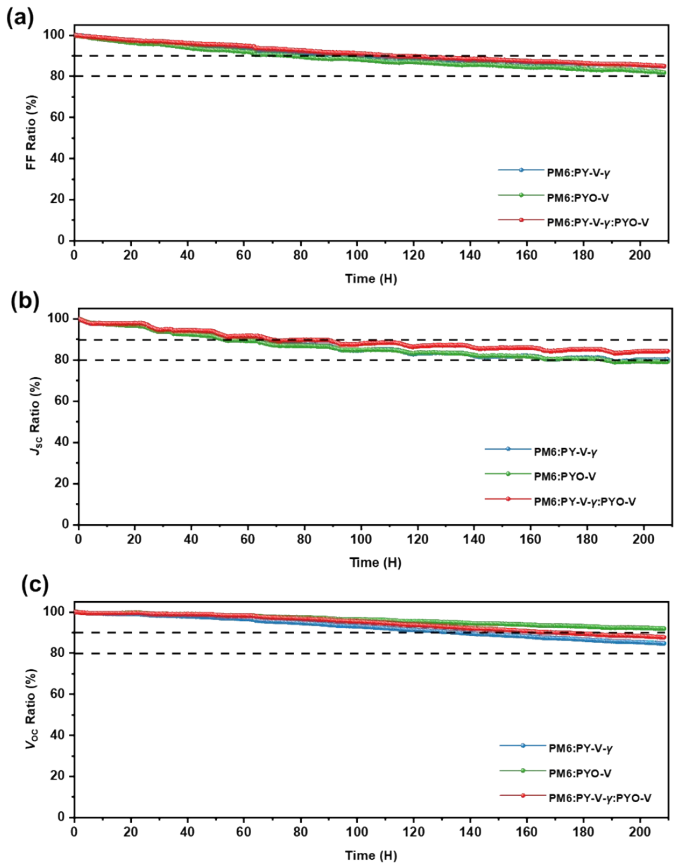

Figure S12. MPPT test of (a)FF; (b) J_{SC} and (c) V_{OC} of the three all-PSCs.

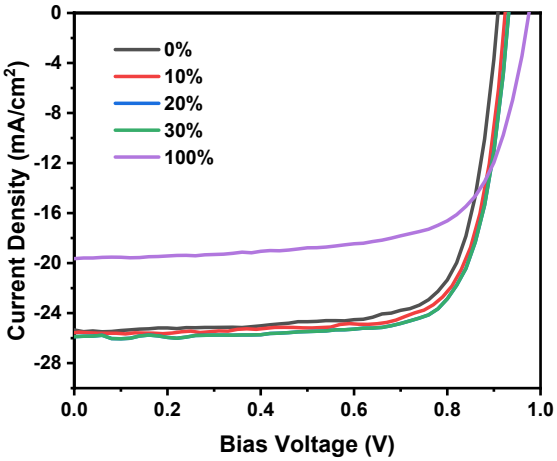

Figure S13. *J-V* characteristic curves of all-PSCs based on PM6:PY-V-*γ* with different third component ratio of PYO-V.

Table S4. Photovoltaic parameters based on PM6:PY-V-*γ* with different third component ratio of PYO-V.

Third component (wt%)	V_{OC} **(V)**	J_{SC} **(mA/cm²)**	**FF (%)**	**PCE (%)**
0	0.909	25.3	75.7	17.4
10	0.924	25.6	75.9	18.0
20	0.932	25.9	76.5	18.5
30	0.948	25.6	73.7	17.9
100	0.975	19.6	69.4	13.3

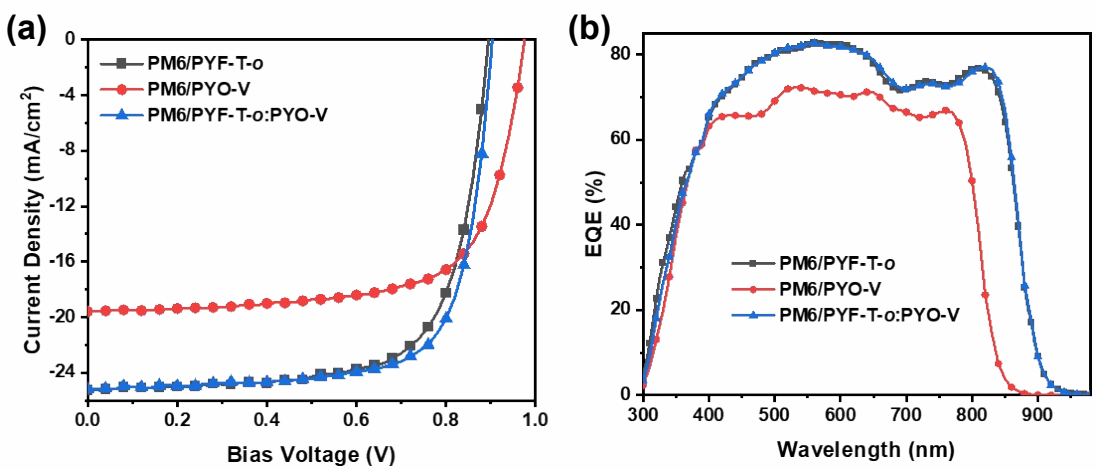

Figure S14. (a) *J-V* characteristic curves of all-PSCs based on PM6:PYF-T-*o*, PM6:PYO-V and PM6:PYF-T-*o*:PYO-V. (c) EQE curves of the devices based on PM6:PYF-T-*o*, PM6:PYO-V and PM6:PYF-T-*o*:PYO-V.

Table S5. Photovoltaic parameters of devices based on the PM6:PYF-T-*o*, PM6:PYO-V and PM6:PYF-T-*o*:PYO-V under the AM 1.5 G illumination of 100 mW cm^{-2}.

active layer	V_{OC} [V]	J_{SC} [mA/cm^2]	J_{EQE} [mA/cm^2]	FF	PCE [%]
PM6:PYF-T-*o*	0.891±0.004 (0.895)	25.2±0.2 (25.27)	24.2	0.702±0.007 (0.704)	15.8±0.1 (15.9)
PM6:PYO-V	0.972±0.002 (0.975)	19.2±0.3 (19.59)	19.0	0.686±0.025 (0.694)	12.8±0.6 (13.3)
PM6:PYF-T-*o*:PYO-V	0.901±0.001 (0.903)	25.3±0.2 (25.2)	24.3	0.725±0.007 (0.734)	16.6±0.1 (16.7)

Synthesis of YO-OD

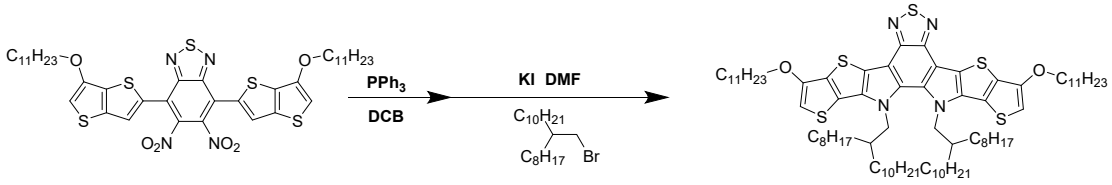

Compound 1 (581 mg, 0.69 mmol) and Triphenylphosphine (2.17g, 8.28 mmol) were dissolved in the 1,2-Dichlorobenzene(o-DCB, 20 mL) under Nitrogen. After being heated at 180 ℃ overnight, the solvent was removed to get the crude product. The brown residue was mixed Potassium carbonate (954 mg, 6.9 mmol) and Potassium iodide (573 mg, 3.45 mmol) in DMF (15 mL) under Nitrogen and heated at 85℃ for 0.5h, following by adding 9-(bromomethyl)nonadecane (2.5g 6.9mmol)and stirred overnight. After cooled down to room temperature, the reaction mixture was quenched by the addition of water and extracted with DCM three times. The combined organic phase was washed with dilute HCl. Then the solution was dried over Na_2SO_4 and concentrated under reduced pressure. The residue was purified by flash column chromatography (n-hexane: DCM= 4:1, v/v) to get the product as yellowish-brown oil (560 mg, 61%).^{1}H NMR (400 MHz, $CDCl_3$) δ 6.29 (s, 2H), 4.57 (d, *J* = 7.6 Hz, 4H), 4.16 (t, *J* = 6.5 Hz, 4H), 2.11 – 2.04 (m, 2H), 1.94 – 1.85 (m, 4H), 1.58 – 0.79 (m, 114H). ^{13}C NMR (101 MHz, $CDCl_3$) δ 150.62, 146.96, 136.22, 131.96, 131.16, 122.45, 121.53, 110.97, 95.00, 70.09, 54.34, 38.02, 31.33, 31.20, 30.99, 29.72, 29.08, 29.06, 29.04, 29.01, 28.95, 28.90, 28.83, 28.77, 28.70, 28.62, 28.56, 25.45, 24.83, 22.10, 22.05, 22.00, 13.54, 13.51. MALDI-TOF MS: calculated for: $C_{80}H_{130}N_4O_2S_5$ (M+), 1340.20; found, 1339.89.

Synthesis of YO-OD-CHO

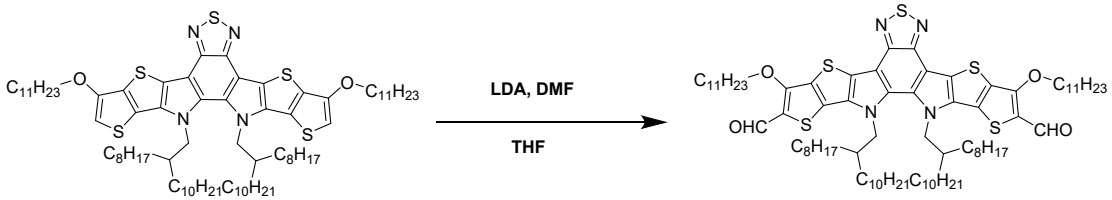

To a dry ice acetylnitrile bath of **YO-OD** (510 mg, 0.38 mmol) in THF (20 mL) under Nitrogen was added dropwise 2.0 M lithium diisopropylamide in THF/Hexane (1.15 mL, 2.28 mmol). After 1 h, the anhydrous *N*, *N*-Dimethylformamide (2 mL) was added and kept stirred for 1 h. Brine was added to quench the reaction and the mixture was extracted with DCM for three times. The combined organic phase was washed with water followed by brine. Then the solution was dried over Na_2SO_4 and concentrated under reduced pressure. The residue was purified by flash column chromatography (n-hexane: DCM= 1.5:1, v/v) to get the product as orange oil (370 mg, 69%).^{1}H NMR (400 MHz, $CDCl_3$) δ 10.12 (s, 2H), 4.69 (t, J = 6.5 Hz, 4H), 4.60 (d, J = 7.5 Hz, 4H),

2.04 (d, J = 5.6 Hz, 2H), 1.99 – 1.90 (m, 4H), 1.62 – 0.79 (m, 114H). ^{13}C NMR (101 MHz, $CDCl_3$) δ 180.39, 157.93, 146.71, 136.05, 132.52, 129.40, 128.70, 127.39, 111.46, 72.56, 54.57, 38.29, 31.28, 31.15, 29.60, 29.28, 29.06, 28.99, 28.95, 28.91, 28.75, 28.71, 28.67, 28.55, 25.17, 24.74, 22.05, 21.97, 13.50, 13.48, 13.47. MALDI-TOF MS: calculated for: $C_{82}H_{130}N_4O_4S_5$ (M+), 1396.27; found, 1395.90

Synthesis of YO-OD-Br

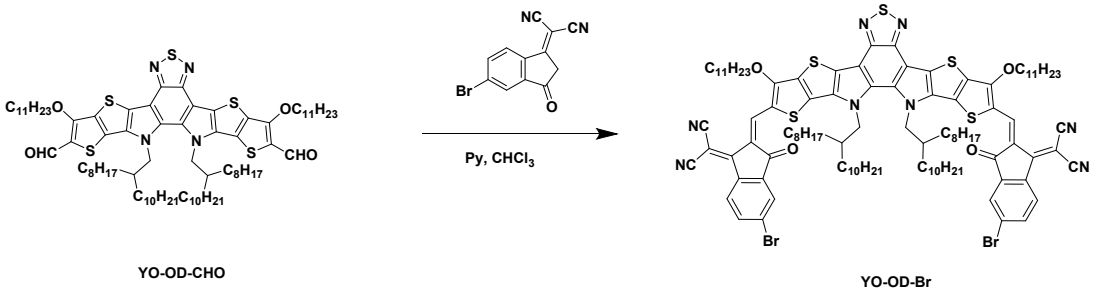

To a mixture of **YO-OD-CHO** (380 mg, 0.272 mmol) and **IC-Br** (298 mg, 1.09 mmol) in anhydrous $CHCl_3$ (20 mL) being heated to 65 °C was added Pyridine (2mL) under Nitrogen. The mixture was refluxed for 4 hours and then being cooled to room temperature, the mixture was poured into CH_3OH (90 mL) and filtered. After removing the solvent, the residue was purified using column chromatography on silica gel (*n*-hexane:DCM= 1:1, v/v), yielding a blue solid (425 mg, 82%). ^{1}H NMR (400 MHz, $CDCl_3$) δ 9.38 (s, 2H), 8.53 (d, *J* = 8.4 Hz, 2H), 7.98 (d, *J* = 1.8 Hz, 2H), 7.82 (dd, *J* = 8.4, 1.7 Hz, 2H), 4.80 (t, *J* = 6.5 Hz, 4H), 4.74 (d, *J* = 7.5 Hz, 4H), 2.08 (d, *J* = 8.8 Hz, 2H), 2.03 (dd, *J* = 14.7, 6.9 Hz, 4H), 1.46 – 0.92 (m, 90H), 0.88 (t, *J* = 6.8 Hz, 10H), 0.81 (dt, *J* = 14.4, 7.1 Hz, 18H). ^{13}C NMR (101 MHz, $CDCl_3$) δ 187.37, 162.33, 159.73, 147.39, 138.67, 138.24, 137.57, 137.18, 134.66, 134.46, 131.82, 128.82, 128.16, 126.39, 126.20, 120.16, 117.87, 115.44, 114.94, 113.04, 74.13, 67.16, 55.67, 44.57, 39.26, 31.94, 31.88, 30.53, 29.83, 29.80, 29.70, 29.66, 29.63, 29.62, 29.57, 29.49, 29.44, 29.39, 29.37, 29.28, 25.82, 25.59, 22.71, 22.66, 15.39, 14.14, 10.86. MALDI-TOF MS: calculated for: $C_{108}H_{136}Br_2N_8O_4S_5$ (M+), 1906.41; found, 1906.78.

Polymerization of **PYO-V**

trans-1,2-bis(tri-nbutylstannyl)ethylene (15.8 mg, 0.026 mmol) and dibrominated monomer YO-OD- Br (49.7 mg, 0.026 mmol), $Pd_2(dba)_3$ (1.5 mg, 1.6×10^{-3} mmol), P(*o*-tol)$_3$ (1.99 mg, 6.4×10^{-3} mmol), and toluene (2 mL) were added to a 25 mL Schlenk tube. The tube was purged and sealed under nitrogen flow and stirred at 115 °C for 3 days. Then the reaction mixture was cooled down to room temperature and precipitated into 20 mL of MeOH. The obtained solid was purified by a size exclusion chromatography column, and then concentrated under reduced pressure. The solid residue was re-dissolved in chloroform (2 mL) and added slowly to methanol (20 mL). The precipitates were collected by filtration, washed with MeOH, and dried in vacuum, leading to a deep blue solid as the product PYO-V (yield: 68%).

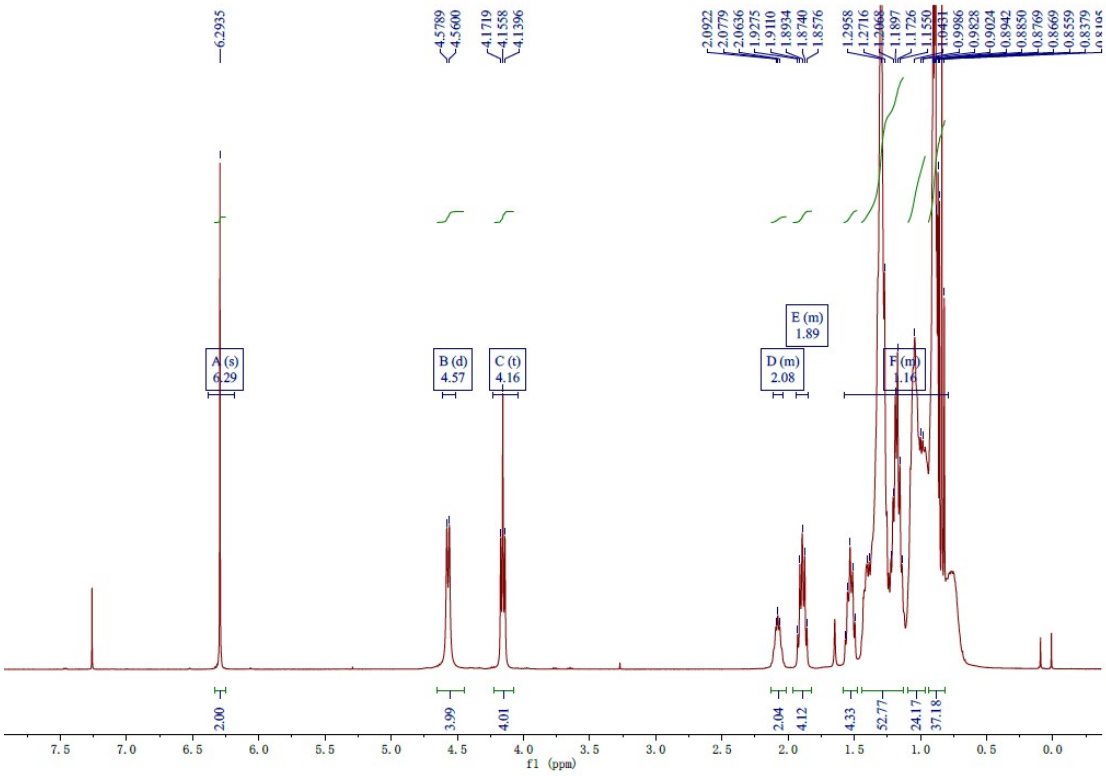

Figure S15. ^{1}HNMR spectrum of **YO-OD** (400 MHz, $CDCl_3$).

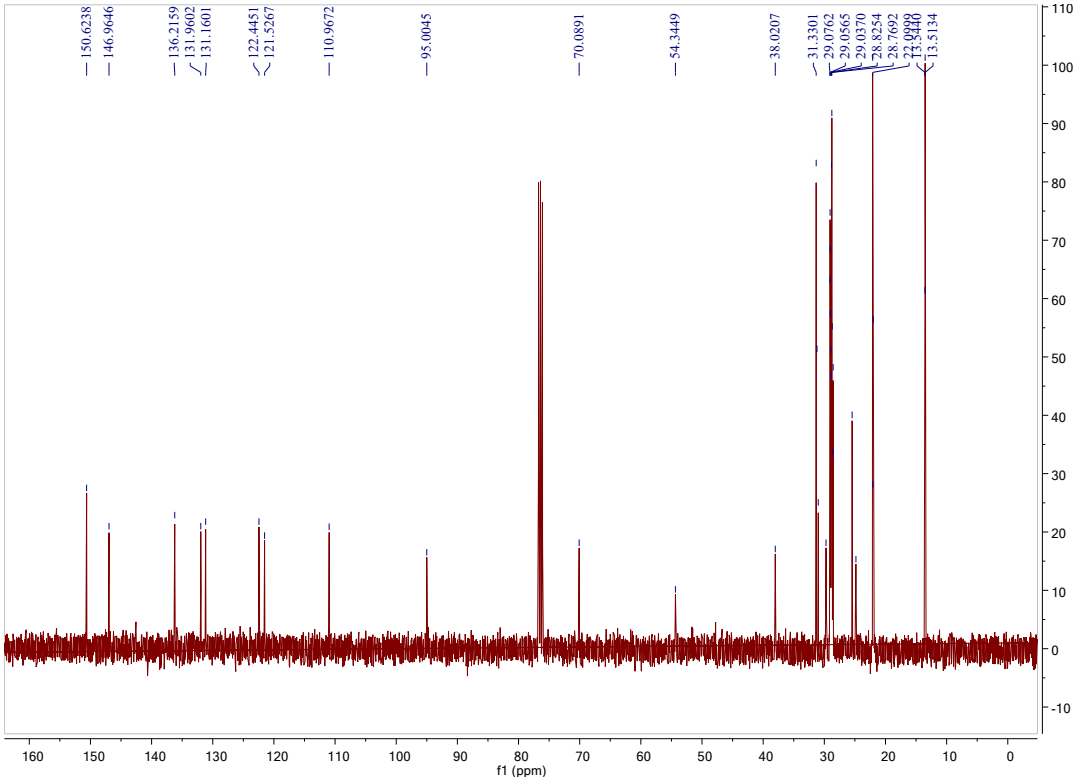

Figure S16. ^{13}CNMR spectrum of **YO-OD** (400 MHz, $CDCl_3$).

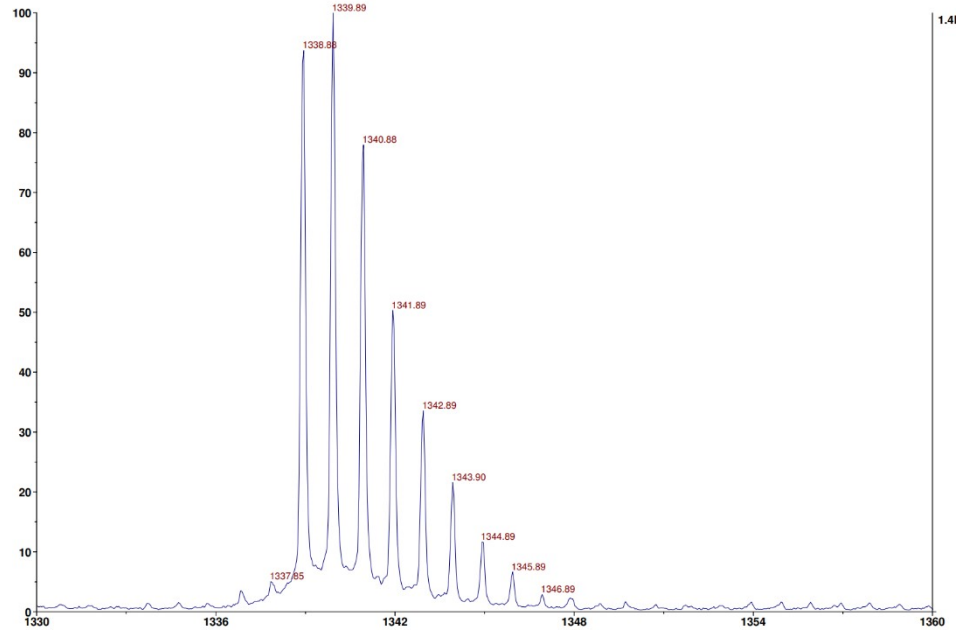

Figure S17. MS spectrum (MALDI-TOF) of compound **YO-OD**.

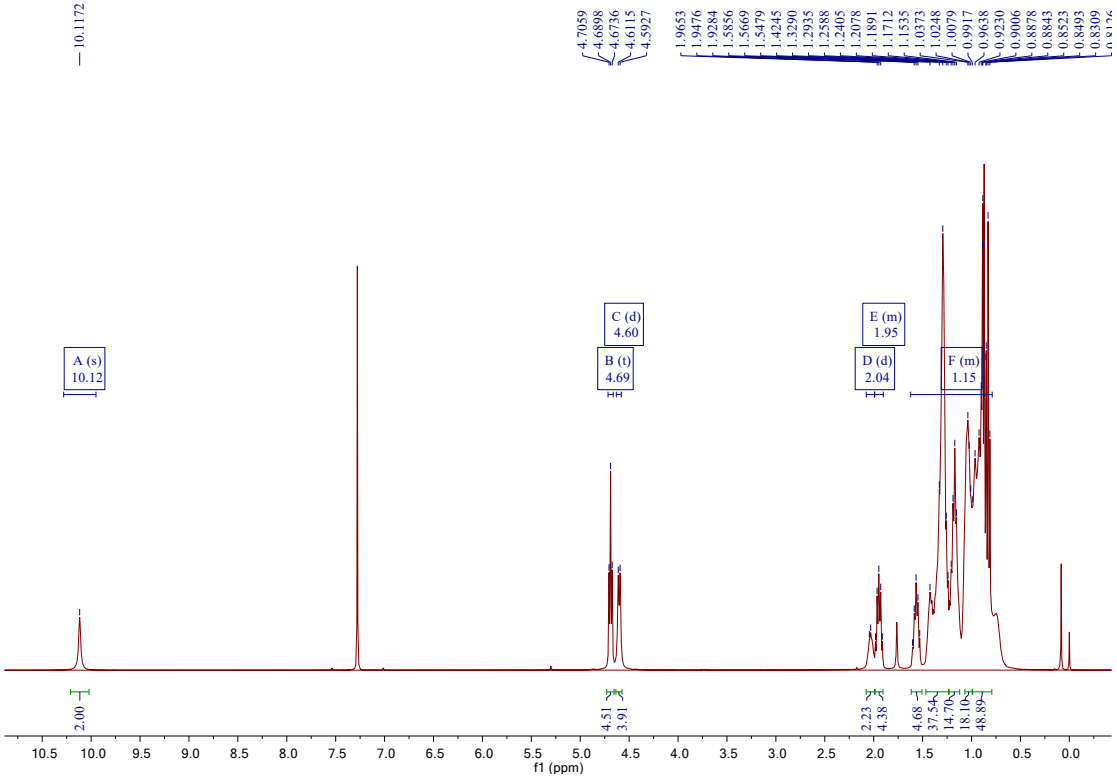

Figure S18. ^{1}HNMR spectrum of **YO-OD-CHO** (400 MHz, $CDCl_3$).

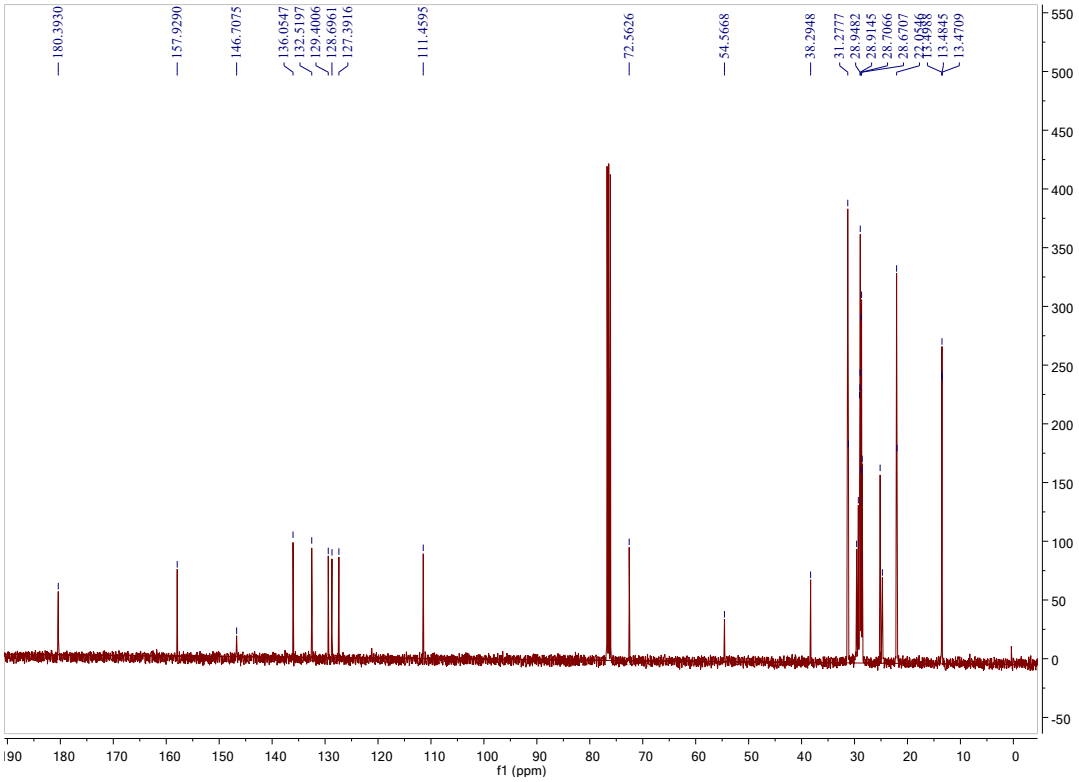

Figure S19. ^{13}CNMR spectrum of **YO-OD-CHO** (400 MHz, $CDCl_3$).

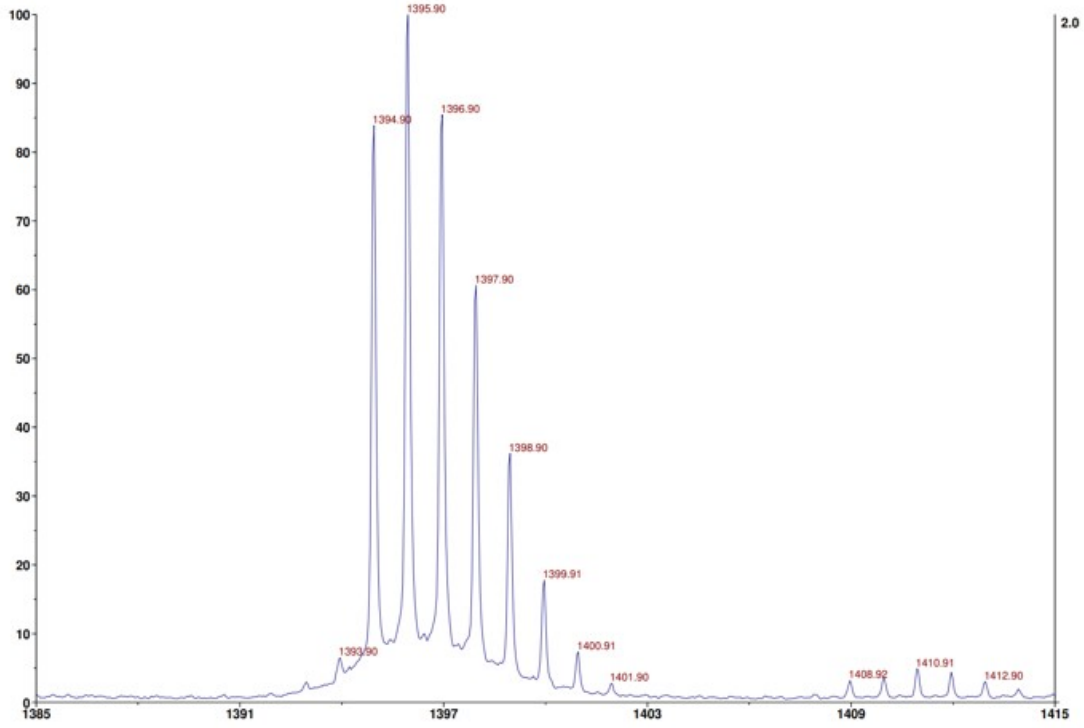

Figure S20. MS spectrum (MALDI-TOF) of compound **YO-OD-CHO**.

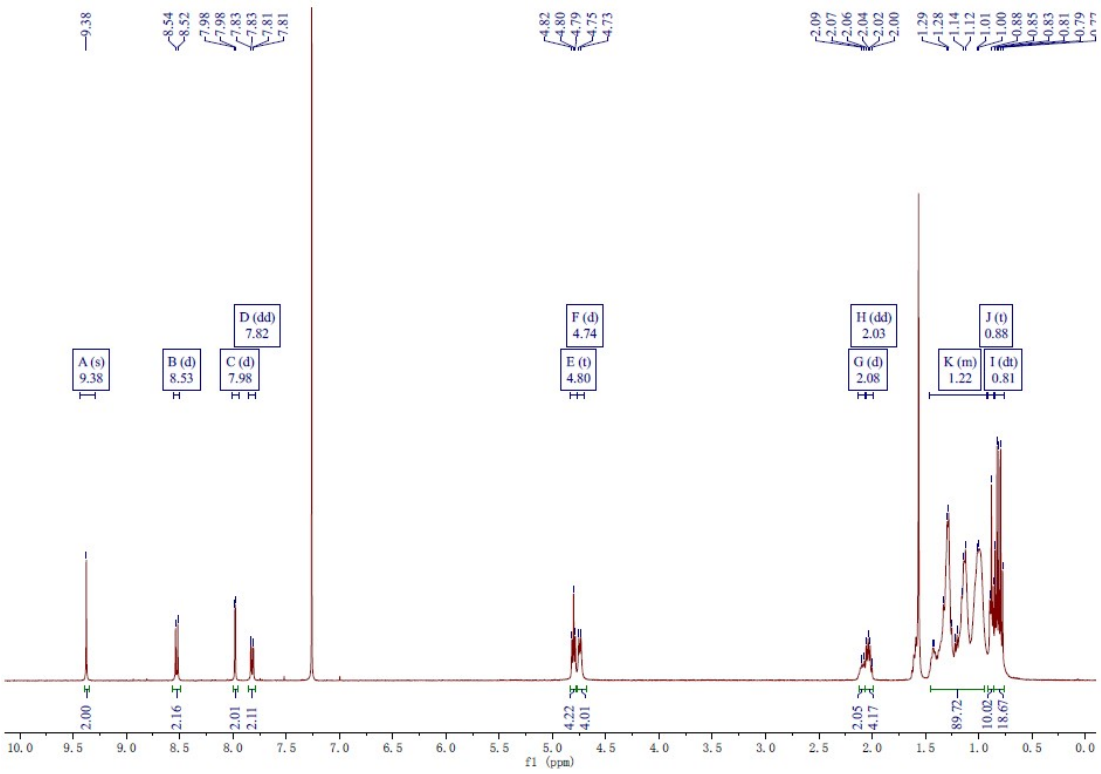

Figure S21. [1]HNMR spectrum of **YO-OD-Br** (400 MHz, $CDCl_3$).

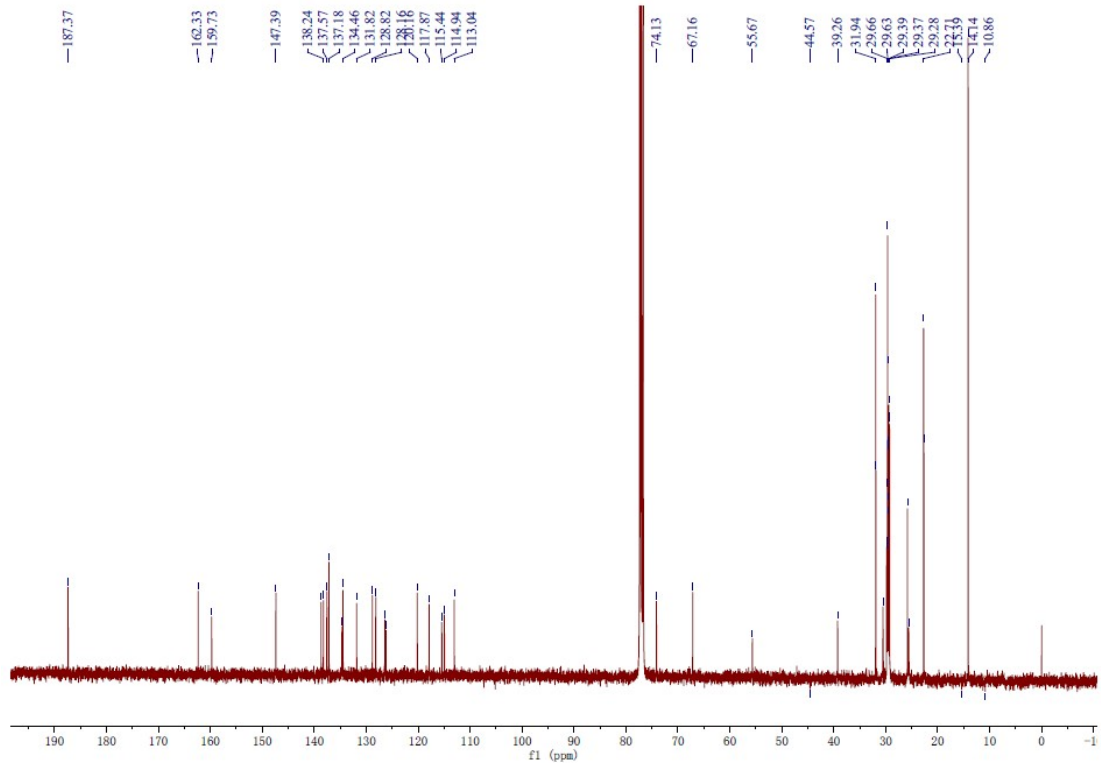

Figure S22. [13]CNMR spectrum of **YO-OD-Br** (400 MHz, $CDCl_3$).

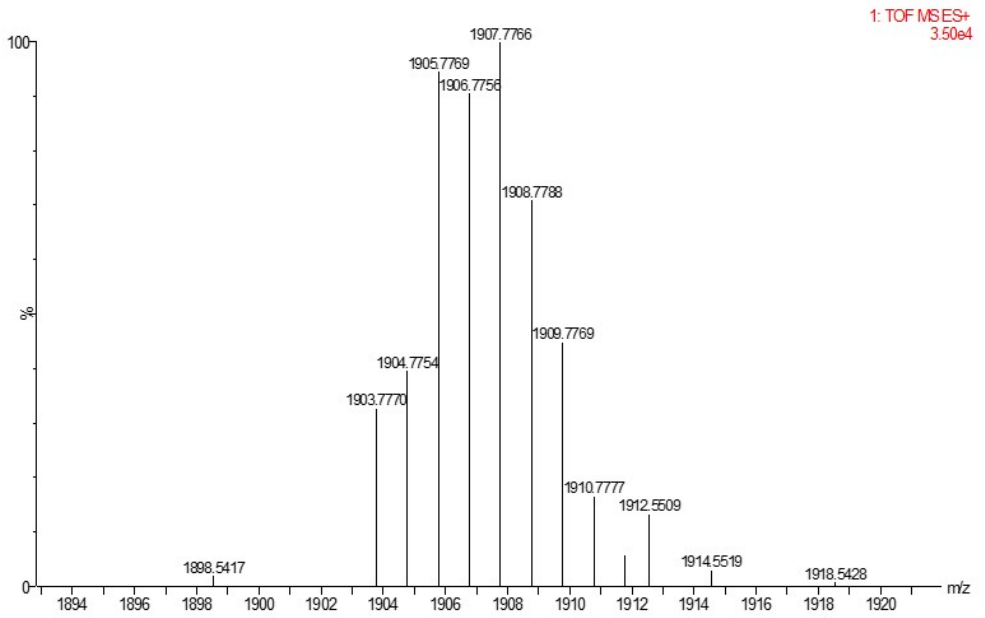

Figure S23. MS spectrum (MALDI-TOF) of compound **YO-OD-Br**.

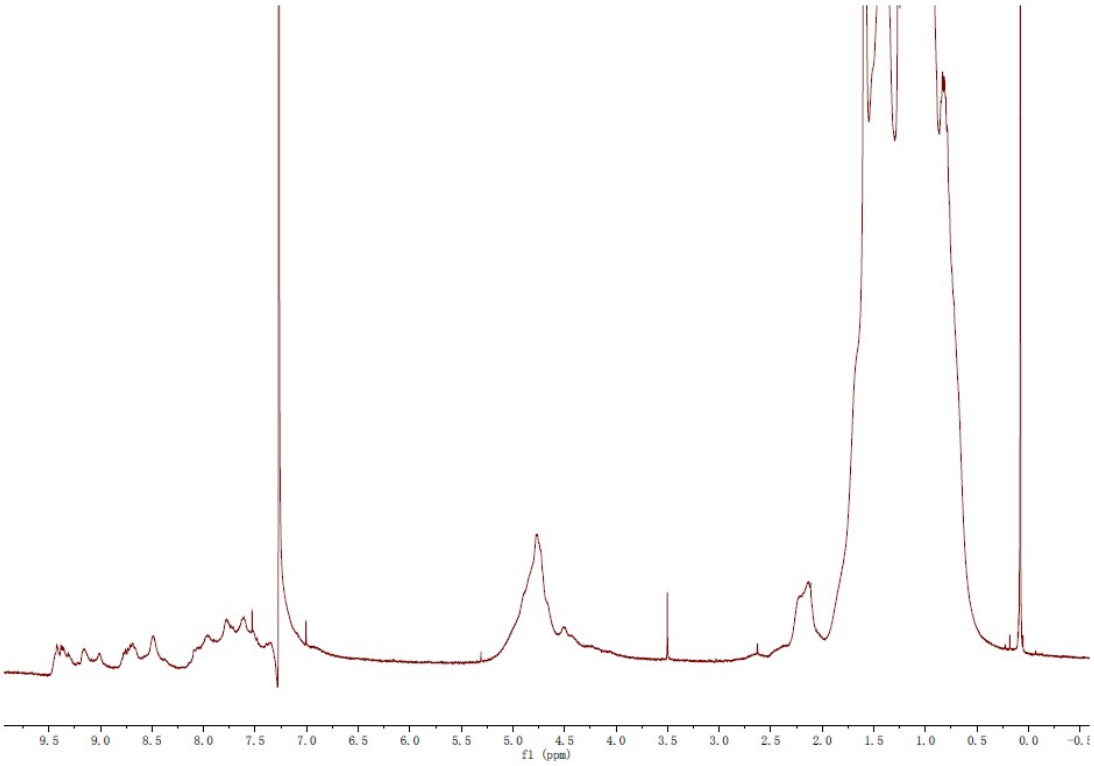

Figure S24. ^{1}HNMR spectrum of **PYO-V** (400 MHz, $CDCl_3$).